

Received July 24, 2019, accepted July 31, 2019, date of publication August 8, 2019, date of current version August 21, 2019.

Digital Object Identifier 10.1109/ACCESS.2019.2933852

Single Wearable Accelerometer-Based Human Activity Recognition via Kernel Discriminant Analysis and QPSO-KELM Classifier

YIMING TIAN^{1,2,3}, JIE ZHANG^{1,2}, (Senior Member, IEEE),
LINGLING CHEN¹, YANLI GENG¹, AND XITAI WANG^{1,3}

¹School of Artificial Intelligence, Hebei University of Technology, Tianjin 300130, China

²School of Engineering, Merz Court, Newcastle University, Newcastle upon Tyne NE1 7RU, U.K.

³Beijing Key Laboratory of Rehabilitation Technical Aids for Old-Age Disability, Key Laboratory of Human Motion Analysis and Rehabilitation Technology of the Ministry of Civil Affairs, National Research Center for Rehabilitation Technical Aids, Beijing 100176, China

Corresponding authors: Jie Zhang (jie.zhang@newcastle.ac.uk) and Xitai Wang (xitaiwang56@gmail.com)

This work was supported in part by the China Scholarship Council under Grant 201806700006, in part by the National Natural Science Foundation of China under Grant 61803143 and Grant 61703135, and in part by the National Key Technology Research and Development Program of the Ministry of Science and Technology of China under Grant 2015BAI06B03.

ABSTRACT In recent years, sensor-based human activity recognition (HAR) has gained tremendous attention around the world with a range of applications. Instead of using body sensor network-based recognition systems which are intrusive and increase equipment cost, we focus on the development of efficient HAR approach based on a single triaxial accelerometer. In order to improve the recognition accuracy of the system, a novel recognition approach based on kernel discriminant analysis (KDA) and quantum-behaved particle swarm optimization-based kernel extreme learning machine (QPSO-KELM) is proposed. KDA is utilized to extract more meaningful features and enhance the discrimination between different activities. To verify the effectiveness of KDA, three kinds of features including original features, linear discriminant analysis (LDA) features and KDA features are extracted and compared for activity recognition. In addition, QPSO-KELM is compared with two existing classification methods: support vector machine (SVM) and extreme learning machine (ELM), which are commonly utilized in activity recognition. Meanwhile, two comparative optimization methods for KELM are also discussed in the experiment. The experimental results demonstrate the superiority of the proposed approach.

INDEX TERMS Human activity recognition, kernel Fisher discriminant analysis, kernel extreme learning machine, quantum-behaved particle swarm optimization, wearable sensor.

I. INTRODUCTION

HAR has become an active research area with a wide range of applications. HAR can automatically recognize activities of daily living by using cameras or inertial sensors and machine learning algorithms. These activities include not only some simple physical activities such as walking, jumping and running but also some complex activities such as cooking and bathing. HAR systems can serve as a medium to obtain information about people's behavior. Thus, it can be widely used for context perception [1], [2], home-based care [3], sports training [4], fall detection [5] and many other applications.

The associate editor coordinating the review of this manuscript and approving it for publication was Mahdi Zareei.

Vision-based HAR has been developed rapidly in recent years. In order to improve recognition reliability, a distributed camera recognition scheme was proposed in [6] for tracking and activity recognition. Huynh-The *et al.* [7] utilized a Kinect camera for analyzing indoor activities. With the development of deep learning techniques, some vision-based HAR methods utilizing convolutional neural networks for feature extraction and activity recognition have been reported [8], [9]. One drawback of these vision-based approaches is that the performance will be greatly affected by external conditions, especially when there is a bad illumination condition. In addition, these vision-based systems are not suitable for installation in some places, such as bathrooms and bedrooms, which may violate personal privacy. Last but not least, as the vision-based systems are always installed

in one location, it is difficult for the system to continuously monitor one particular user when the user is not within the visual range.

With the development of micro-electromechanical techniques, inertial sensing devices with small size, low power consumption and light weight have been continuously applied in various digital products, such as mobile phones and tablet computers. Therefore, in recent years, sensor-based HAR has attracted more attentions from researchers. Sensor-based HAR systems can be divided into two categories: single sensor-based systems and body sensor network-based systems. The body sensor network-based activity recognition system has been designed for badminton training [10], gait analysis [11] and crowd sensing [12]. In addition, in order to gain a tradeoff among computational complexity and accuracy, Cao *et al.* [13] reported optimizing the multi-sensor network layout by ensemble pruning. Though body sensor network-based activity recognition system can improve the generalization performance, this approach is not suitable for long-term use in real life because multiple sensors increase the risk of sensor drop, which can cause system failures if the system is designed with data and feature level fusion. In addition, this approach increases the cost of the system and can cause inconvenience to the user's activities. Therefore, more and more researches have been focused on single sensor-based systems. Cheng and Jhan [14] utilized a single triaxial accelerometer for fall detection and investigated four positions on human body for placing the accelerometer. Margarito *et al.* [15] analyzed the performance of the template matching method on activity recognition by using single accelerometer placed on the wrist. Wang *et al.* [16] compared the power of triaxial accelerometer and triaxial gyroscope which were utilized in recognizing six human physical activities by using a smartphone attached to the waist. Rodríguez-Martín *et al.* [17] dealt with posture transitions recognition of Parkinson's disease (PD) patients by using a triaxial accelerometer. A HAR method using a single inertial sensor placed at the waist was proposed in [18]. Different features are extracted from accelerometer and gyroscope data. Feature vectors constructed by feature level fusion are utilized to recognize six activities with back propagation algorithm.

High-quality features are critical to the performance of the HAR system, especially for single sensor-based implementation. Useful features should be extracted from the original inertial signals in order to not only reduce computation time but also increase recognition accuracy. For acceleration signals, there are mainly three kinds of feature extraction methods, including time domain method, frequency domain method and time-frequency domain method. The time domain features can provide better computational time and efficiency for HAR systems. Time domain features such as the mean, the standard deviation and the correlation coefficient are utilized in most studies [19]. The fast Fourier transform is a commonly used time-frequency conversion method. Common frequency domain features are energy,

fast Fourier transform (FFT) coefficients and spectral density. Wavelet analysis which can decompose inertial data into detail and approximation signals with different precisions has been widely used to perform the time-frequency analysis.

A number of state-of-the-art classification models have been utilized for HAR. Awais *et al.* [20] utilized the SVM as a classifier to develop and validate the proposed inertial sensors-based physical activity classification system for older adults. Four major activities of daily living including sitting, standing, walking and lying were recognized by SVM. In [21], k nearest neighbors (KNN) method is utilized as a classifier in a novel time series-based HAR method. Neural networks show the best performance among five machine learning algorithms when recognizing construction workers' eight different activities in [22]. However, artificial neural network requires large training examples and its performance can be limited by the lack of training examples. These popular learning techniques often have challenging problems in HAR, such as slow learning, high computation time and poor generalization performance. The recently developed ELM as a single hidden layer feed-forward neural network has the advantages of fast running speed and good generalization performance and it has been widely utilized in HAR [23], [24]. The drawback of ELM is that the recognition performance is obviously affected by the algorithm parameters. Meanwhile, the randomly generated input weights and hidden layer biases of ELM can make the algorithm unstable.

Considering these drawbacks of ELM, KELM [25], [26] was proposed on the basis of ELM and kernel functions. KELM is a kind of machine learning algorithm with strong stability and generalization ability. Some researches demonstrated that the generalization and recognition performance of KELM is better than those of the SVM algorithm and the ELM algorithm. However, due to the existence of kernel functions, the performance of KELM is greatly affected by kernel parameters. Therefore, this paper utilizes the QPSO algorithm [27] with better convergence performance to optimize the KELM parameters to improve the performance of the recognition system.

Some features may be irrelevant or redundant and the feature set that contains these redundant features may increase computation time and reduce classifier's performance. Moreover, due to the complexity of human physical activity, the activities include simple activities (such as standing, sitting and walking) and more complex ones (such as eating, bathing and brushing teeth). Some features which may be effective for recognizing simple activities may perform poorly in distinguishing some complex types of activities. Principal component analysis (PCA) [28], [29] and LDA [30] are commonly applied in researches to reduce the feature vectors and select the most distinguishing features. KDA [31] is a non-linear generalized kernel form of LDA. It solves the LDA problem in a high-dimensional feature space, which produces a set of nonlinear discriminant vectors as new features. In this paper, we will introduce KDA to extract more

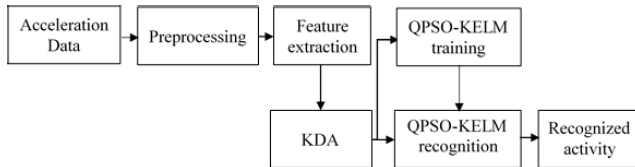


FIGURE 1. The workflow of the proposed HAR approach.

meaningful features of the activities and integrate it with QPSO-KELM classifier to achieve improved recognition performance.

The rest of the paper is organized as follows. The proposed activity recognition approach is detailed in Section II, where the workflow, experimental acquisition equipment, data acquisition and preprocessing, feature extraction method, KDA, and the QPSO-KELM classifier are presented in detail. Experimental results are presented in Section III. Finally, conclusions of this study are drawn in Section IV.

II. THE PROPOSED APPROACH

Figure 1 shows the workflow of the proposed activity recognition approach. The approach mainly involves four steps: data acquisition and preprocessing, features extraction from each sliding window, feature transformation by KDA, QPSO-KELM training and recognition.

A. WEARABLE COMPONENT

The TRIGNO™ wireless system from Delsys Company is utilized for collecting the dataset in the experiment. The device contains a data acquisition platform and a data collection node which are respectively shown in Figure 2(a) and Figure 2(b). The model of the acquisition platform is SP-W02 and the model of data collection node is SP-W01D. The data collection node integrates a triaxial accelerometer and an EMG sensor. The sampling frequency of the integrated triaxial accelerometer is 150Hz with an acceleration range of $\pm 6G$ with resolution = 0.063 (G is the gravitational constant). In this study, we only used triaxial acceleration signal for the experiments. Since the data collection node has wireless transmission function, the acceleration signal can be transmitted to the data acquisition platform. Once the data acquisition platform receives the activity data, the activity data will be transmitted and stored in the computer system, as shown in Figure 2(c).

B. DATA ACQUISITION AND PREPROCESSING

Five healthy students including 3 males and 2 females participated in the collection of experimental data. The data collection node is bind to each participant's waist, as shown in Figure 3. All participants are required to wear the data collection node at the same position for six daily activities, including walking, running, going upstairs, going downstairs, jumping and standing. They performed each activity twice. Figure 4 shows the acceleration signals of “walking”

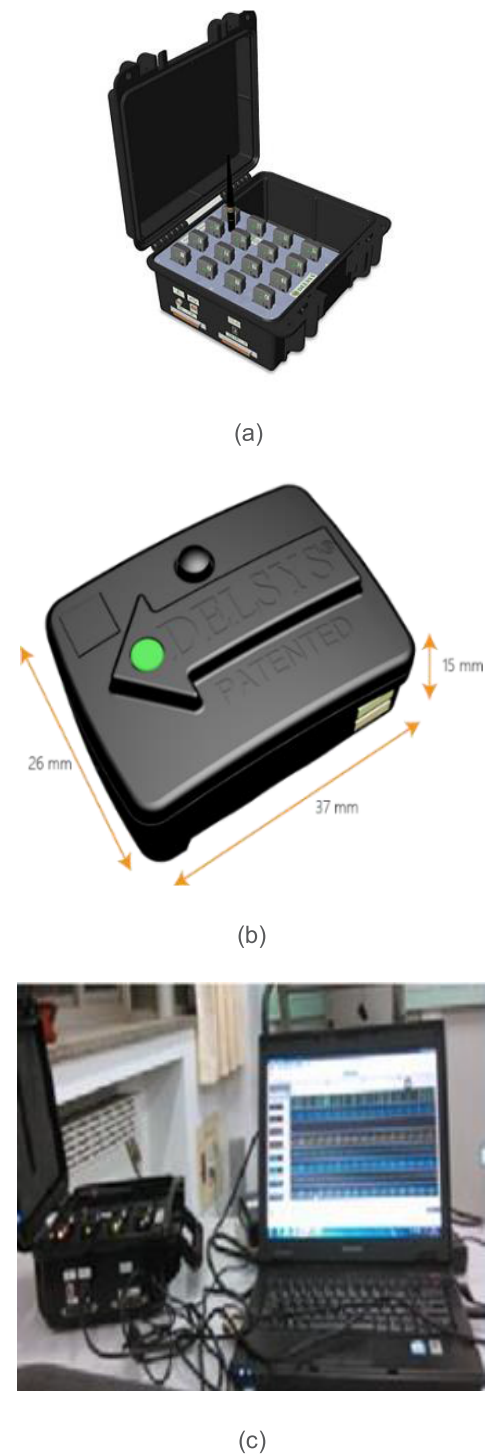


FIGURE 2. Human activity data acquisition platform based on acceleration sensor: (a) the data acquisition platform, (b) data collection node containing the triaxial accelerometer, (c) experimental data acquisition process.

and “going upstairs” for the triaxial accelerometer. After preprocessing operations such as removing abnormal data points, the sliding window is utilized to divide the data into windows with equal length. Some studies of HAR have proved that the sliding windows of 1-2 seconds

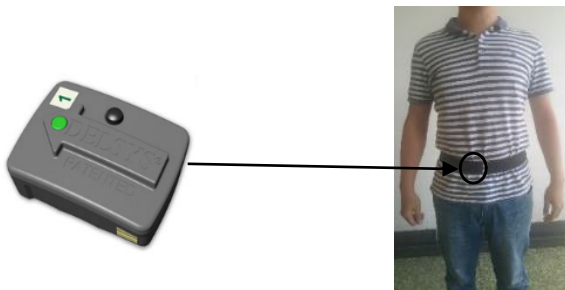


FIGURE 3. The binding position of the data collection node.

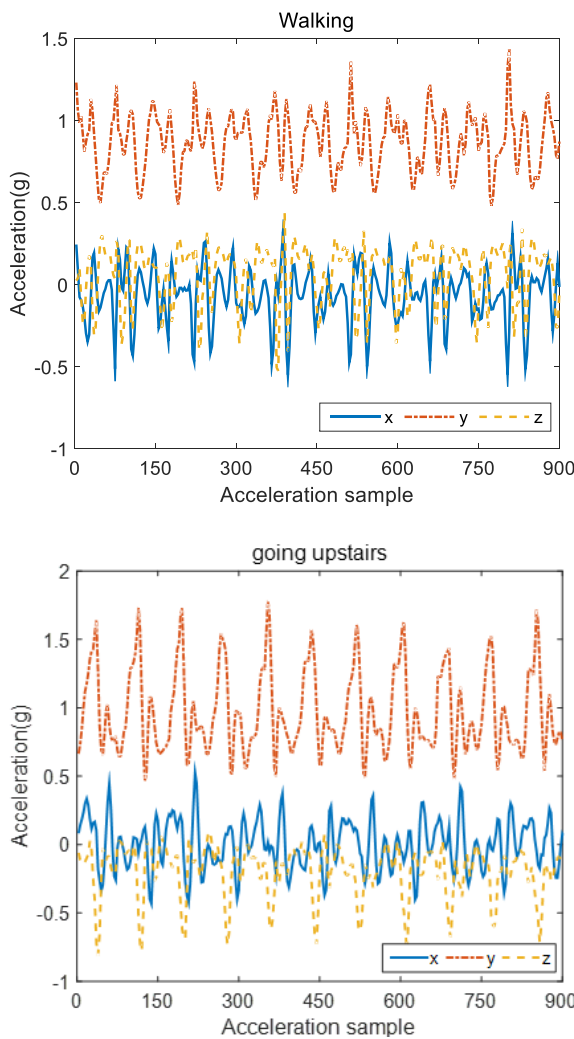


FIGURE 4. The acceleration data of “walking” and “going upstairs”.

are more effective in HAR [32]. Therefore, we selected a sliding window of 2s that containing 300 data points for extracting characteristic data. To prevent the loss of information between adjacent windows, we choose the sliding window with 50% overlap, which has been widely utilized in HAR. Finally, we obtained 100 samples of each activity type for each participant. All the activity samples of the

TABLE 1. Extracted features.

Mean	Standard deviation	Skewness
Correlation between axes	Maximum	Minimum
Signal magnitude area(SMA)	FFT coefficient	Wavelet energy

five participants constituted the entire data set for feature extraction.

C. FEATURE EXTRACTION

A large set of features have been extracted from the raw acceleration signal and are listed in Table 1. A brief description of each feature is given as follows.

The standard deviation σ is the square root of the variance of the acceleration data and skewness S measures the direction and extent of deflection of the acceleration data distribution:

$$\sigma = \sqrt{\frac{1}{N} \sum_{i=1}^N (a_i - \bar{a})^2} \quad (1)$$

$$S = \frac{1}{N} \sum_{i=1}^N \left(\frac{a_i - \bar{a}}{\sigma} \right)^3 \quad (2)$$

where a_i is the acceleration data with $i = 1, 2, \dots, N$, N is the number of samples, $\bar{a} = \frac{1}{N} \sum_{i=1}^N a_i$ is the mean of N acceleration data.

The interquartile range (IQR) is the difference between the 3rd quartile Q_3 and the 1st quartile Q_1 . The acceleration data a_i is sorted from small to large as b_i , $i = 1, 2, \dots, N$. The position of the quartile is $P_j = 1 + (N - 1)j/4$, $j = 1, 2, 3$ is the number of quantiles, k_j is the integer part and r_j is the fractional part of P_j . The quartile Q_j and the interquartile range IQR are calculated according to:

$$Q_j = b_{k_j} + (b_{k_j} + 1 - b_{k_j})r_j$$

$$\text{IQR} = Q_3 - Q_1 \quad (3)$$

The cross-correlation coefficient C is the ratio of the covariance of the 2-axis acceleration to the standard deviation product of the 2-axis acceleration. For example, the cross-correlation coefficient C_{xy} of the x -axis and y -axis acceleration is calculated by:

$$C_{xy} = \text{cov}(x, y) / (\sigma_x \sigma_y) \quad (4)$$

where $\text{cov}(x, y)$ is the covariance of the x and y axis acceleration, σ_x and σ_y are the standard deviations of the x and y axis acceleration respectively.

The signal magnitude area (SMA) is calculated by:

$$\text{SMA} = \sum_{i=1}^N (|x(i)| + |y(i)| + |z(i)|) \quad (5)$$

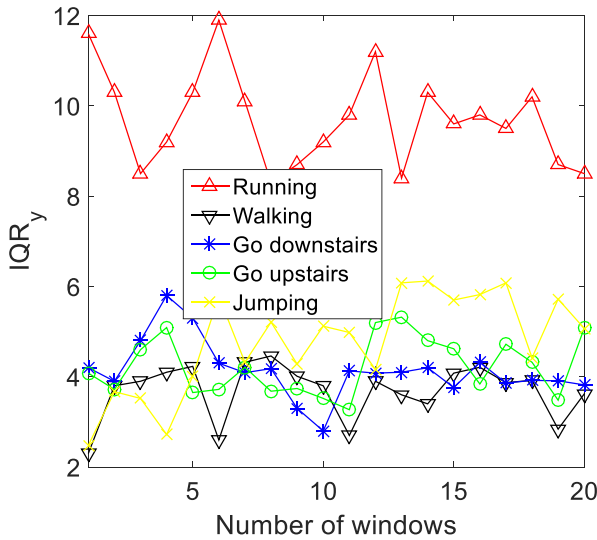


FIGURE 5. The IQR_y distribution of five activities.

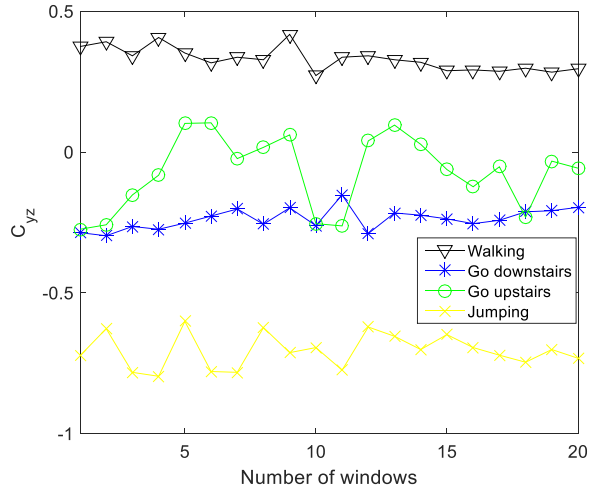


FIGURE 6. The C_{yz} distribution of four activities.

where $x(i)$, $y(i)$ and $z(i)$ respectively indicates the values of x -axis, y -axis and z -axis acceleration signals at the i th sampling point.

The FFT coefficient is extracted by FFT analysis of the triaxial acceleration signal to extract frequency information from 1 to 50 Hz. We utilize db3 as the wavelet function and the triaxial acceleration signals are decomposed into 4 levels, wavelet energy features are the sum of the squared detail coefficients of level 3 and level 4.

Figures 5 and 6 show the distribution of two kinds of feature, IQR_y and C_{yz} , for different activities respectively. As can be seen from Figure 5, the IQR_y can effectively separate the running from other activities. However, there are many crossovers of the IQR_y among the other four activities and it is difficult to distinguish them. As can be seen from Figure 6, C_{yz} enhances the discrimination of the above four indistinguishable activities, but there are still some crossovers of IQR_y between “go upstairs” and “go downstairs”. Therefore, KDA is utilized in this paper to enhance the discrimination between similar activities.

D. KERNEL FISHER DISCRIMINANT ANALYSIS

LDA is a supervised dimensionality reduction and classification technology developed in the field of pattern recognition. The main idea of LDA is to find the optimal projection matrix by using the Fisher criterion. It can maximize the inter-class dispersion of the projection of the test data while minimizing intra-class dispersion. KDA is a nonlinear extension of LDA. It seeks nonlinear discriminating feature space by nonlinear feature mapping. The kernel Fisher discriminant analysis is briefly described as follows:

Suppose that all sample points in the p -dimensional space have C classes: G_1, G_2, \dots, G_C , and the total number of samples is N . The j th ($j = 1, 2, \dots, C$) class G_j contains N_j samples written as $x_j^1, x_j^2, \dots, x_j^{N_j}$.

The sample $x \in R^p$ passes through the nonlinear high-dimensional mapping ϕ and the corresponding mode $\phi(x) \in H$. In the high-dimensional feature space H , the intra-class dispersion S_W and the inter-class dispersion S_B of the training samples are given by Eq(6) and Eq(7) respectively:

$$S_W = \frac{1}{N} \sum_{i=1}^C \sum_{j=1}^{N_i} [\phi(x_i^j) - \mathbf{m}_i] [\phi(x_i^j) - \mathbf{m}_i]^T \quad (6)$$

$$S_B = \frac{1}{N} \sum_{i=1}^C N_i (\mathbf{m}_i - \mathbf{m})(\mathbf{m}_i - \mathbf{m})^T \quad (7)$$

where \mathbf{m}_i represents the i th sample mean in the feature space H : $\mathbf{m}_i = (1/N_i) \sum_{j=1}^{N_i} \phi(x_i^j)$ and \mathbf{m} represents the mean of all sample points in the feature space H : $\mathbf{m} = (1/N) \sum_{i=1}^C \sum_{j=1}^{N_i} \phi(x_i^j)$. In the feature space H , the Fisher criterion is:

$$J(\mathbf{w}) = \max \frac{\mathbf{w}^T S_B \mathbf{w}}{\mathbf{w}^T S_W \mathbf{w}} \quad (8)$$

where \mathbf{w} is any non-zero column vector. The Fisher discriminant finds the best projection vector \mathbf{w} by optimizing Eq (8). Since the feature space H dimension is too high, \mathbf{w} cannot be directly obtained, thus the following kernel function is introduced.

$$k(x, z) = \langle \phi(x), \phi(z) \rangle \quad (9)$$

Eq (9) indicates that any two inner product vectors in the high dimensional space H can be represented by a kernel function. Then the optimal solution \mathbf{w} in Eq (8) can be expressed as $\mathbf{w} = \sum_{i=1}^N \alpha_i \phi(x_i)$, where $\alpha = (\alpha_1, \alpha_2, \dots, \alpha_N)^T$ is a column vector. So in the high-dimensional feature space H , the Fisher criterion can be expressed as:

$$J(\boldsymbol{\alpha}) = \max \frac{\boldsymbol{\alpha}^T S_B \boldsymbol{\alpha}}{\boldsymbol{\alpha}^T S_W \boldsymbol{\alpha}} = \max \frac{\boldsymbol{\alpha}^T \mathbf{K}_B \boldsymbol{\alpha}}{\boldsymbol{\alpha}^T \mathbf{K}_W \boldsymbol{\alpha}} \quad (10)$$

In the formula, \mathbf{K}_B and \mathbf{K}_W are calculated as follows:

$$\left\{ \begin{array}{l} \mathbf{K}_B = \frac{1}{C(C-1)} \sum_{i=1}^C \sum_{j=1}^C (\boldsymbol{\mu}_i - \boldsymbol{\mu}_j)(\boldsymbol{\mu}_i - \boldsymbol{\mu}_j)^T \\ \boldsymbol{\mu}_i = \left[\frac{1}{N_i} \sum_{j=1}^{N_i} k(x_1, x_i^j), \dots, \frac{1}{N_i} \sum_{j=1}^{N_i} k(x_N, x_i^j) \right]^T \\ \mathbf{K}_W = \frac{1}{C} \sum_{i=1}^C \frac{1}{N_i} \sum_{j=1}^{N_i} (\boldsymbol{\xi}_j - \boldsymbol{\mu}_j)(\boldsymbol{\xi}_j - \boldsymbol{\mu}_j)^T \\ \boldsymbol{\xi}_j = (k(x_1, x_j), k(x_2, x_j), \dots, k(x_N, x_j))^T \end{array} \right.$$

Therefore, the problem in Eq (10) is transformed into maximizing $\mathbf{K}_W^{-1} \mathbf{K}_B$ and its corresponding eigenvector. In practical applications, \mathbf{K}_W is often not guaranteed to be non-singular. Therefore, $\mathbf{K}_W + \sigma \mathbf{I}$ is often used to replace \mathbf{K}_W , where σ is a small positive number (usually $\sigma = 10^{-7}$). In this paper, the RBF kernel function is used:

$$k(x, z) = \exp(-\frac{\|x - z\|^2}{\delta^2}) \quad (11)$$

In Eq(11), the parameter δ is positive and the selection of δ is an optimization problem. In this study, the cross-validation method is used to select the parameter δ based on our previous research [33]. Figure 7 shows the 3-D feature plots for the four activities by using the original features, LDA features and KDA features. In Figure 7(a), x_1 is the minimum of the z -axis, x_2 is the value of C_{xy} and x_3 is the mean of the y -axis. In Figure 7(b) and 7(c), x_1, x_2 and x_3 are three features randomly selected from the LDA features and KDA features, respectively.

It can be seen from Figure 7 that the original feature samples have many intersections in the feature space and it is difficult to distinguish different activity types. For the LDA features, the samples belonging to the same activity become spatially aggregated and the samples of different activity types are gradually dispersed, but there are still large overlaps among some activities, such as going upstairs, going downstairs and jumping. After the KDA operation, the overlapping samples are further reduced and the sample distribution of different types of activity samples tends to be independent.

E. KERNEL EXTREME LEARNING MACHINE

As a single hidden layer feed-forward neural network (SLFN), ELM was proposed by Huang *et al.* [34] in 2006. It has good generalization ability and does not need to iteratively adjust the network weights, which greatly improves the training speed. KELM extends ELM from explicit activation to implicit mapping functions. It shows better generalization performance than the traditional ELM algorithm in many research areas. KELM is described as follows:

For any N different samples (\mathbf{x}_j, t_j) , $j = 1, 2, \dots, N$, where $\mathbf{x}_j = [x_{j1}, x_{j2} \dots x_{jn}]^T$ is the j th sample, each sample

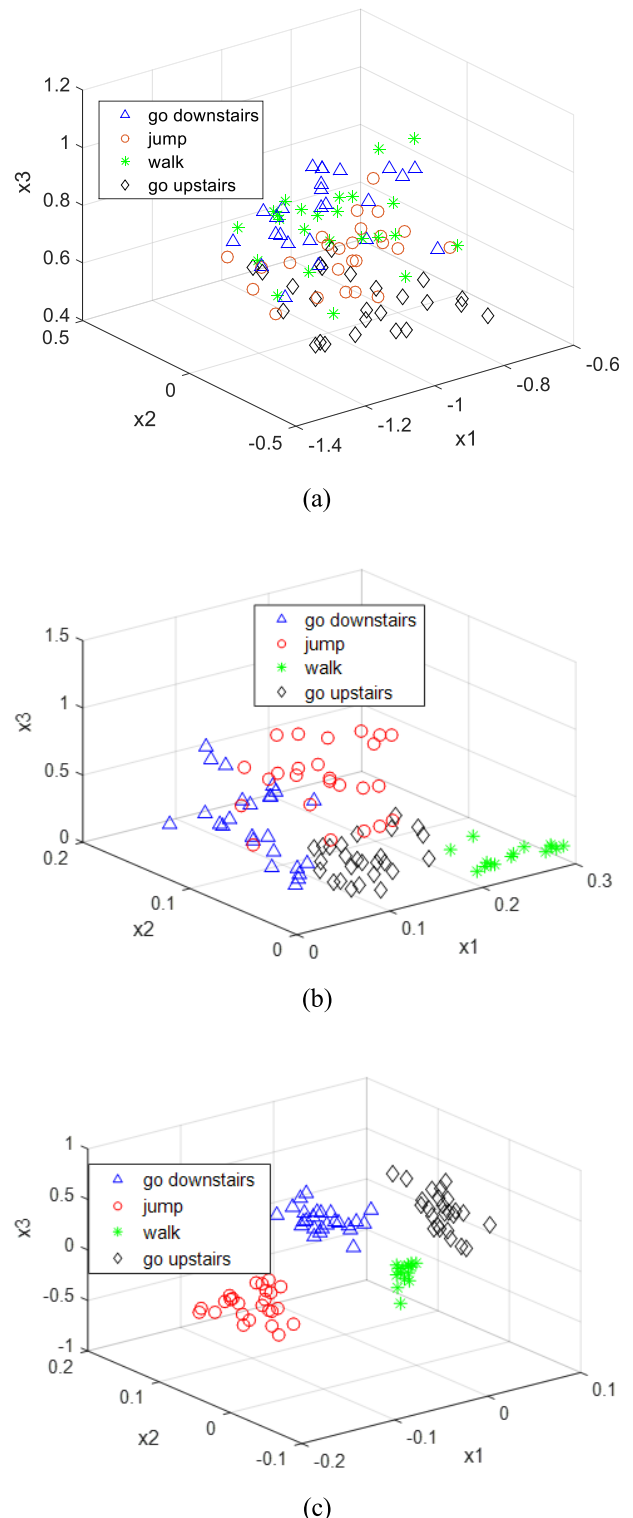


FIGURE 7. 3-D feature plots for three kinds of features (a) 3-D feature space representation of original features; (b) 3-D feature space representation for LDA implementation on original features; (c) 3-D feature space representation for KDA implementation on original features.

contains n -dimensional features, and $\mathbf{t}_j = [t_{j1}, t_{j2}, \dots, t_{jm}]^T$ is the encoded class label. All samples belong to m different classes, and the ELM mathematical model with L hidden

neurons can be expressed as:

$$\sum_{i=1}^L \beta_i g(\mathbf{w}_i \cdot \mathbf{x}_j + b_i) = \mathbf{t}_j, \quad j = 1, 2, \dots, N \quad (12)$$

where $g(x)$ is the excitation function, \mathbf{w}_i , b_i , and β_i are the input weights, hidden layer bias and output weights of the i th hidden neuron node respectively. Equation (12) can be written in matrix form:

$$\mathbf{H}\boldsymbol{\beta} = \mathbf{T} \quad (13)$$

where $\boldsymbol{\beta}$ represents the vector of output layer weights, \mathbf{T} is the corresponding coding class label, and \mathbf{H} is the hidden layer output matrix:

$$\mathbf{H} = \begin{bmatrix} g(\mathbf{w}_1 \cdot \mathbf{x}_1 + b_1) & \dots & g(\mathbf{w}_L \cdot \mathbf{x}_1 + b_L) \\ \vdots & \dots & \vdots \\ g(\mathbf{w}_1 \cdot \mathbf{x}_N + b_1) & \dots & g(\mathbf{w}_L \cdot \mathbf{x}_N + b_L) \end{bmatrix}_{N \times L} \quad (14)$$

Since Eq(13) is linear, $\boldsymbol{\beta}$ is obtained by the following equation:

$$\boldsymbol{\beta} = \mathbf{H}^\dagger \mathbf{T} \quad (15)$$

where \mathbf{H}^\dagger is the generalized inverse matrix of \mathbf{H} . In order to further improve the generalization ability of ELM, Huang *et al.* [35] introduced a kernel function to avoid the problem of ELM method randomly generating input weight and bias values. The calculation formula of KELM output layer weights is as follows:

$$\boldsymbol{\beta} = \mathbf{H}^T (\frac{1}{C} + \mathbf{H}\mathbf{H}^T)^{-1} \mathbf{T} \quad (16)$$

where C is regularization coefficient. The output function for the SLFN is:

$$f(\mathbf{x}_j) = h(\mathbf{x}_j)\boldsymbol{\beta} = h(\mathbf{x}_j)\mathbf{H}^T (\frac{1}{C} + \mathbf{H}\mathbf{H}^T)^{-1} \mathbf{T} \quad (17)$$

where $h(\mathbf{x}_j)$ is the output of the hidden nodes and actually maps the data from input space to the hidden layer feature space \mathbf{H} . When the hidden layer function $h(\mathbf{x}_j)$ is unknown, the kernel function matrix is calculated as follows:

$$\Omega_{\text{ELM}} = \mathbf{H}\mathbf{H}^T : \Omega_{\text{ELM},ij} = h(\mathbf{x}_i) \cdot h(\mathbf{x}_j) = K(\mathbf{x}_i, \mathbf{x}_j) \quad (18)$$

where $K(\mathbf{x}_i, \mathbf{x}_j)$ represents the kernel function. In this paper, the most commonly utilized Gaussian kernel function was applied. Then the output function of KELM can be written as:

$$f(\mathbf{x}) = \begin{bmatrix} K(\mathbf{x}, \mathbf{x}_1) \\ \vdots \\ K(\mathbf{x}, \mathbf{x}_N) \end{bmatrix}^T (1/C + \Omega_{\text{ELM}})^{-1} \mathbf{T} \quad (19)$$

F. USING QPSO TO SELECT THE PARAMETERS OF KELM

The setting of the parameters of KELM will have a great influence on its generalization performance. In order to obtain the optimal parameters of the KELM, we optimize C in Eq (19) and the parameters of the kernel function by QPSO. The dimension of the searching space corresponds to the number of parameters to be optimized and the position of each particle represents a set of optimized parameter values. Some studies have proved that the standard particle swarm optimization (PSO) algorithm cannot guarantee global convergence and, in order to overcome this shortcoming, Sun *et al.* [36] introduced quantum mechanics and proposed the QPSO algorithm. The QPSO algorithm utilizes the wave function $\Psi(X, k)$ to describe the state of each particle. The evolution equation is:

$$X_{k+1}^i = X_k^p \pm \beta |Ck - X_k^i| \ln \frac{1}{u} \quad (20)$$

where $X_k^p = \varphi P_k^i + (1-\varphi)G_k$ is a random position between P_k^i and G_k , P_k^i is the best position of particle i at the k th iteration, $i = 1, 2, \dots, N$. N is the population size, G_k is the global best position of the population at the k th evolutionary iteration, $C_k = \frac{1}{N} \sum_{i=1}^N P_k^i$ represents the mean of the best individual positions of the k th iteration of all particles, u and φ are random numbers that are uniformly distributed in the range $(0, 1)$, β is a contraction-expansion coefficient and the value is linearly reduced from 1 to 0.5. The specific steps of QPSO-KELM are described as follows:

Step 1: The raw data set is normalized to the range of $[0, 1]$ and define the maximize iterations $K = 200$ and population size $N = 50$.

Step 2: Set $k = 1$. Initialize the position and local optimal position of each candidate particle, as well as global best position of the swarm.

Step 3: Calculate each particle's fitness value according to the fitness function by Eq (20) and update the best-known positions and global best position. The fitness function of the QPSO in the optimization process is the Q -fold cross-validation recognition accuracy ($Q = 5$), which is:

$$F = \frac{1}{Q} \sum_{l=1}^Q \frac{x_{lr}}{x_{lr} + x_{lw}} \quad (21)$$

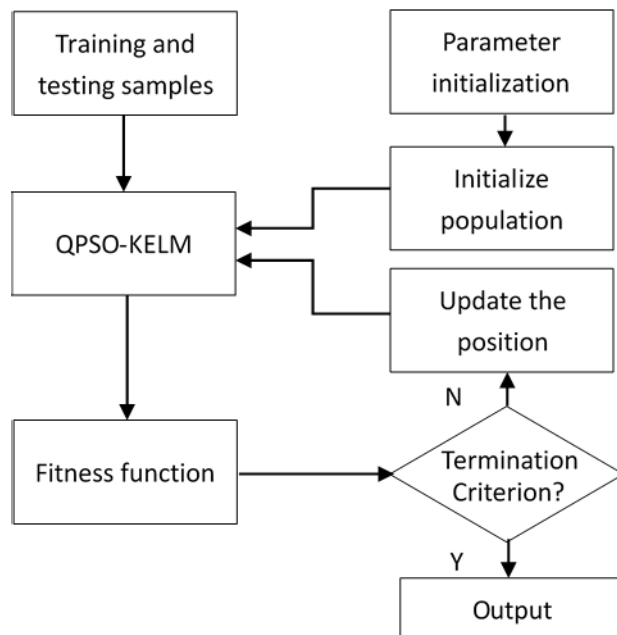
where x_{lr} and x_{lw} are the number of samples correctly and incorrectly recognized in the l th verification sample set of KELM respectively. The larger the fitness value, the better the optimization effect.

Step 4: Update the position of each candidate particle in each iteration, which can be obtained by Equation (19).

Step 5: Set $k = k + 1$. If the maximum iteration is reached, go to Step 6; otherwise, go to Step 3.

Step 6: Export the optimized KELM classifier for recognizing new activity samples.

The flowchart of this procedure is shown in Figure 8.

**FIGURE 8.** Diagram of QPSO for optimizing KELM.

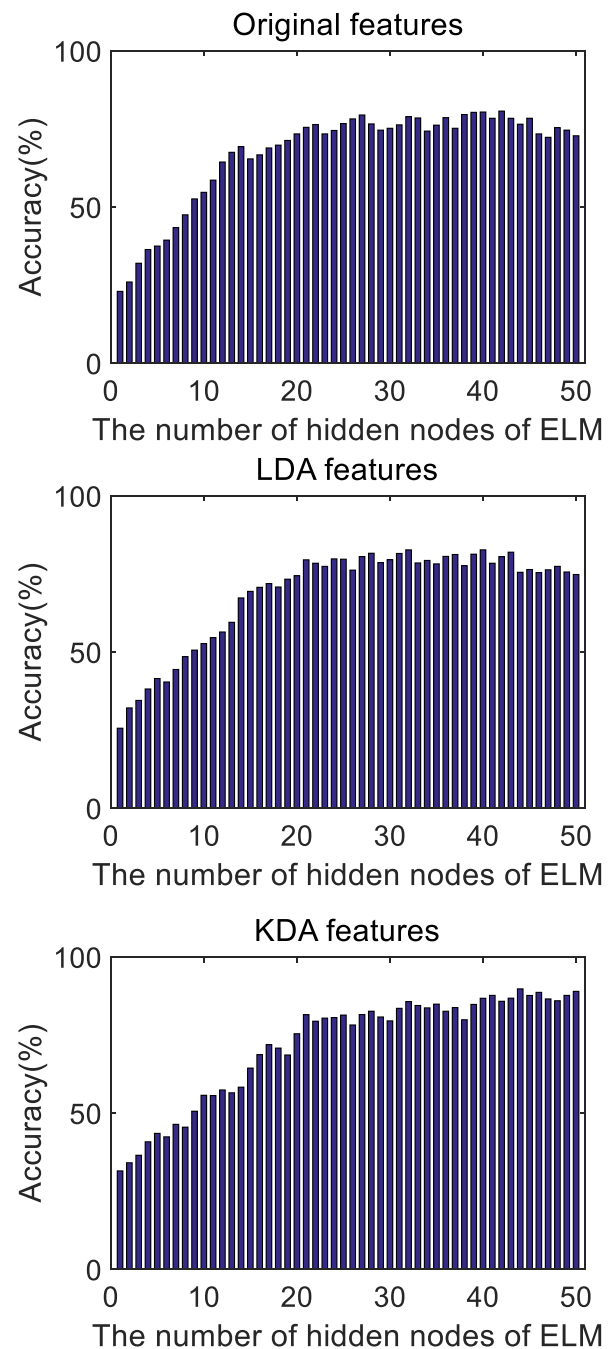
III. RESULTS AND DISCUSSIONS

The leave-one-out (LOO) method is utilized to train and validate the proposed system. The validation was repeated five times. In each experiment, a sample set of one subject is selected as the test data, the sample set of the remaining four subjects constitutes the training data. The final results shown are the average of the five test results. The original features and LDA features are utilized for comparison with KDA features. In addition, another two classification methods ELM and SVM which are very commonly utilized in activity recognition are applied for comparison with KELM. Since the input weights and hidden layer bias values of ELM can be set randomly, the parameter that affects its performance is only the number of hidden neurons. In general, the number of hidden neurons is obtained by the trial and error method. Therefore, In order to get better ELM performance, 50 experiments were carried out with the number of hidden neurons of ELM ranging from 1 to 50.

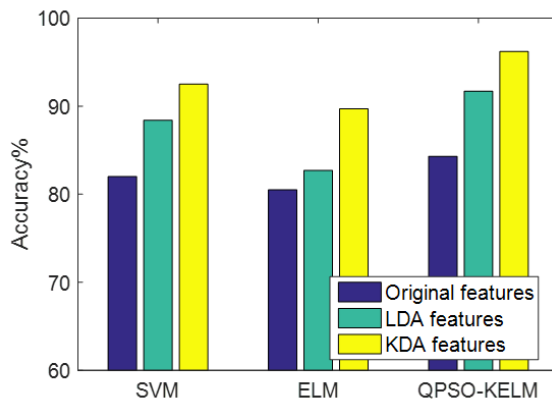
Figure 9 shows the recognition accuracy of the ELM using the three kinds of features when the number of hidden nodes in the hidden layer range from 1 to 50. It can be clearly seen from Figure 9 that the recognition accuracy gradually improves with the increase of the number of hidden nodes. Moreover, due to different kinds of features, the number of hidden nodes when the ELM reaches the optimal performance is also different. It can be seen from Figure 9 that the number of hidden layer nodes is 42, 40 and 44 when ELM obtains the best performance of 80.7%, 82.7% and 89.7% using original features, LDA features and KDA features respectively. This can be used as a basis for optimization of ELM performance.

A. PERFORMANCE COMPARISON OF DIFFERENT FEATURE EXTRACTION METHODS

In order to verify the superiority of the KDA features for distinguishing different activities, three kinds of classifiers

**FIGURE 9.** The performances of ELM when the number of hidden nodes range from 1 to 50.

namely ELM, SVM and QPSO-KELM are utilized to perform comparative experiments with original features and LDA features. The kernel function of KELM is set to Gaussian kernel. For the original features, LDA features and KDA features, the number of hidden neurons in the ELM is set to 42, 40 and 44 respectively, according to their performances, as shown in Figure 9. To optimize SVM performance, experiments with training data show that linear kernels are effective for cross-validation and the parameters of the regularization term are selected by grid search with cross validation of training data.

**FIGURE 10.** Accuracy comparison of three kinds of features.**TABLE 2.** Confusion matrix of SVM based on original features.

	W	R	GU	GD	J	S
W	86	6	2	2	2	2
R	3	82	5	4	4	2
GU	2	3	79	6	7	3
GD	4	3	7	74	9	3
J	2	3	9	7	77	2
S	2	1	1	1	1	94
Total accuracy				82%		

TABLE 3. Confusion matrix of SVM based on LDA features.

	W	R	GU	GD	J	S
W	92	3	2	2	1	0
R	3	91	2	3	1	0
GU	2	3	85	7	2	1
GD	3	1	6	84	6	0
J	2	1	8	6	83	0
S	2	1	1	0	1	95
Total accuracy				88.4%		

Figure 10 shows the accuracy comparison of the three kinds of features when ELM, SVM and QPSO-ELM classifier is utilized. It can be seen from Figure 10 that the KDA features achieve the highest recognition accuracy regardless of the classifier used, which can demonstrate the effectiveness of the KDA features. Additionally, in order to gain a better insight into the discrimination effect of the KDA features and make a comparison with the original features and LDA features, the corresponding confusion matrixes were constructed. Tables 2 to 10 show the confusion matrixes of the three kinds of features and the three classification methods. In Tables 2 to 10, the codes of “W”, “R”, “GU”, “GD”, “J” and “S” represent the activity walking, running, going upstairs, going downstairs, jumping and standing, respectively.

As can be seen from Tables 2 to 10 that using the original features is prone to misrecognition between different

TABLE 4. Confusion matrix of SVM based on KDA features.

	W	R	GU	GD	J	S
W	96	1	1	2	0	0
R	1	95	2	1	0	1
GU	1	2	87	4	5	1
GD	1	2	2	91	3	1
J	1	2	4	3	90	0
S	1	1	1	1	0	96
Total accuracy				92.5%		

TABLE 5. Confusion matrix of ELM based on original features.

	W	R	GU	GD	J	S
W	82	8	4	2	2	2
R	6	83	5	4	3	2
GU	2	4	76	10	7	1
GD	5	3	11	74	7	1
J	2	3	10	7	77	1
S	3	2	2	1	1	91
Total accuracy				80.5%		

TABLE 6. Confusion matrix of ELM based on LDA features.

	W	R	GU	GD	J	S
W	84	8	2	2	2	2
R	5	84	5	4	2	0
GU	2	3	79	9	6	1
GD	4	3	9	77	7	0
J	2	2	9	7	79	1
S	2	1	2	1	1	93
Total accuracy				82.7%		

TABLE 7. Confusion matrix of ELM based on KDA features.

	W	R	GU	GD	J	S
W	94	3	1	1	1	0
R	2	91	3	2	2	0
GU	1	2	88	7	2	0
GD	3	1	6	84	6	0
J	2	1	8	6	83	0
S	1	0	1	0	0	98
Total accuracy				89.7%		

activities, no matter what type of classifier is used. Compared with the original features, the LDA features have improved the discrimination between activities, but the effect of the improvement of discrimination is not obvious. The KDA features can improve the discrimination between different

TABLE 8. Confusion matrix of QPSO-KELM based on original features.

	W	R	GU	GD	J	S
W	85	6	4	2	2	1
R	4	87	3	2	2	1
GU	2	4	80	7	6	1
GD	4	3	8	79	6	0
J	2	3	8	5	81	1
S	2	1	1	1	1	94
Total accuracy				84.3%		

TABLE 9. Confusion matrix of QPSO-KELM based on LDA features.

	W	R	GU	GD	J	S
W	95	1	2	1	1	0
R	1	94	3	1	0	1
GU	1	2	87	4	5	1
GD	2	2	5	88	3	0
J	1	2	5	3	89	0
S	1	1	0	1	0	97
Total accuracy				91.7%		

activities than the original features and the LDA features. By using the KDA features, the number of misrecognitions of activity by the three kinds of classifiers is significantly reduced. In addition, in the performance comparison of classifiers using the same kind of feature, it can be seen that QPSO-KELM can always perform better than the other two classifiers regardless of the types of feature.

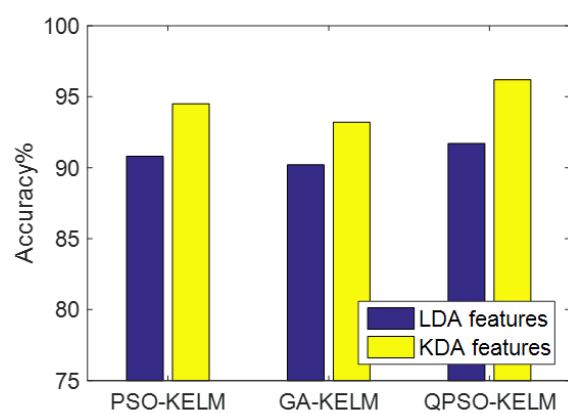
B. PERFORMANCE COMPARISON OF DIFFERENT OPTIMIZATION METHODS FOR KELM

In addition, we also utilize another two optimization methods to verify the superiority of the proposed QPSO-KELM when the KDA features are considered. The PSO and genetic algorithm (GA) are investigated and utilized to optimize the parameters of KELM. And their performances will be compared with QPSO-KELM. In order to ensure the fairness of the comparison, for GA and PSO, the maximum number of iterations and population size are also 200 and 50, respectively, which are the same as QPSO. For the three optimization methods, the optimization range of parameter C and the kernel parameter of the Gaussian kernel function are the same.

Figure 11 shows the accuracy comparison of these three optimization methods for KELM when LDA features and KDA features are utilized. It can be seen from Figure 11 that QPSO-KELM achieves 91.3% and 96.2% accuracy when using LDA features and KDA features respectively, while the other two optimization methods for KELM perform poorly compared with proposed QPSO-KELM. PSO-KELM achieves 90.8% and 94.5% accuracy when using LDA

TABLE 10. Confusion matrix of QPSO-KELM based on KDA features.

	W	R	GU	GD	J	S
W	99	1	0	0	0	0
R	2	96	2	1	0	0
GU	1	0	95	2	2	0
GD	1	2	3	93	1	0
J	0	1	3	1	95	0
S	1	0	0	0	0	99
Total accuracy					96.2%	

**FIGURE 11.** Accuracy comparison of three optimization methods for KELM.**TABLE 11.** Confusion matrix of PSO-KELM based on LDA features.

	W	R	GU	GD	J	S
W	95	1	2	1	1	0
R	2	92	1	3	1	1
GU	1	3	87	5	2	1
GD	1	3	6	86	4	0
J	2	2	5	3	88	0
S	1	1	0	1	0	97
Total accuracy					90.8%	

features and KDA features respectively. GA-KELM achieves only 90.2% and 93.2% accuracy when LDA features and KDA features are utilized respectively. In addition, it can be seen from Figure 11 that the KDA features can significantly improve the accuracy of the KELM compared to the application of the LDA features, no matter which optimization method is used. Tables 11 to 14 show the confusion matrixes of the two optimization methods for KELM when LDA features and KDA features are utilized.

By comparing the confusion matrixes of QPSO-KELM in Tables IX to X and the confusion matrixes of KELMs based on the other two optimization methods in Tables 11 to 14, it can be seen that the QPSO-KELM classifier proposed in this paper can significantly reduce the number of misrecognized samples especially for activities of “running”

TABLE 12. Confusion matrix of PSO-KELM based on KDA features.

	W	R	GU	GD	J	S
W	97	1	1	1	0	0
R	1	96	1	2	0	0
GU	1	2	93	2	1	1
GD	1	2	2	92	2	1
J	1	3	1	2	93	0
S	1	1	1	0	1	96
Total accuracy			94.5%			

TABLE 13. Confusion matrix of GA-KELM based on LDA features.

	W	R	GU	GD	J	S
W	95	1	2	1	1	0
R	1	91	3	2	2	1
GU	2	4	83	4	5	2
GD	1	2	5	89	3	0
J	1	2	6	4	87	0
S	2	1	0	1	0	96
Total accuracy			90.2%			

TABLE 14. Confusion matrix of GA-KELM based on KDA features.

	W	R	GU	GD	J	S
W	96	1	2	1	0	0
R	1	95	1	2	0	1
GU	1	2	90	2	4	1
GD	2	1	2	92	2	1
J	1	2	3	4	90	0
S	1	1	1	1	0	96
Total accuracy			93.2%			

and “going upstairs”. The PSO-KELM, GA-KELM, and QPSO-KELM classifiers achieved recognition accuracy of 90.8%, 90.2% and 91.7% when LDA features are utilized, respectively. PSO-KELM, GA-KELM and QPSO-KELM classifiers achieved recognition accuracy of 93.2% 94.5% and 96.2 when KDA features are utilized, respectively. It can be clearly concluded that the proposed approach based on KDA features and QPSO-KELM classifier achieves the highest recognition accuracy among three kinds of features and the above classification models.

IV. CONCLUSION

In this paper, a HAR approach based on KDA features and QPSO-KELM classifier is proposed to improve the performance of a single triaxial accelerometer based HAR. The ELM, SVM and QPSO-KELM classifiers are utilized to evaluate the introduced KDA features. Compared with the original features and LDA features, the introduced KDA features have been validated in enhancing the discrimination between activities. In addition, this paper also compares the

performances of KELM classifiers optimized by PSO, GA and QPSO methods and proves that the proposed QPSO-KELM model can achieve higher accuracy on the original features, LDA features and KDA features. Experimental results show that the proposed approach can improve the recognition accuracy effectively. In the future, more subjects and more complex activities will be required to test KDA features and proposed QPSO-KELM classifier. Moreover, the datasets from different body positions will be considered for verifying the proposed approach.

REFERENCES

- [1] W. M. Ismail, M. M. Hassan, and H. A. Alsalamah, “Context-enriched regular human behavioral pattern detection from body sensors data,” *IEEE Access*, vol. 7, pp. 33834–33850, 2019.
- [2] R. Fernandez-Rojas, A. Perry, H. Singh, B. Campbell, S. Elsayed, R. Hunjet, and H. A. Abbass, “Contextual awareness in human-advanced-vehicle systems: A survey,” *IEEE Access*, vol. 7, pp. 33304–33328, 2019.
- [3] A. Chelli and M. Pätzold, “A machine learning approach for fall detection and daily living activity recognition,” *IEEE Access*, vol. 7, pp. 38670–38687, 2019.
- [4] Z. Wang, J. Wang, H. Zhao, S. Qiu, J. Li, F. Gao, and X. Shi, “Using wearable sensors to capture posture of the human lumbar spine in competitive swimming,” *IEEE Trans. Hum.-Mach. Syst.*, vol. 49, no. 2, pp. 194–205, Apr. 2019.
- [5] S. K. Gharghan, S. L. Mohammed, A. Al-Naji, M. J. Abu-AlShaeer, H. M. Jawad, A. M. Jawad, and J. Chahl, “Accurate fall detection and localization for elderly people based on neural network and energy-efficient wireless sensor network,” *Energies*, vol. 11, no. 11, 2018, Art. no. 2866.
- [6] B. Song, A. T. Kamal, C. Soto, S. Ding, J. A. Farrell, and A. K. Roy-Chowdhury, “Tracking and activity recognition through consensus in distributed camera networks,” *IEEE Trans. Image Process.*, vol. 19, no. 10, pp. 2564–2579, Oct. 2010.
- [7] T. Huynh-The, C.-H. Hua, N. A. Tu, T. Hur, J. Bang, D. Kim, M. B. Amin, B. H. Kang, H. Seung, S.-Y. Shin, E.-S. Kim, and S. Lee, “Hierarchical topic modeling with pose-transition feature for action recognition using 3D Skeleton data,” *Inf. Sci.*, vol. 444, pp. 20–35, May 2018.
- [8] M. Munoz-Organero, “Human activity recognition based on single sensor square HV acceleration images and convolutional neural networks,” *IEEE Sensors J.*, vol. 19, no. 4, pp. 1487–1498, Feb. 2019.
- [9] Y. Kim and B. Toomajian, “Hand gesture recognition using micro-Doppler signatures with convolutional neural network,” *IEEE Access*, vol. 4, pp. 7125–7130, 2016.
- [10] Z. Wang, M. Guo, and C. Zhao, “Badminton stroke recognition based on body sensor networks,” *IEEE Trans. Hum.-Mach. Syst.*, vol. 46, no. 5, pp. 769–775, Oct. 2016.
- [11] Z. Wang, S. Qiu, Z. Cao, and M. Jiang, “Quantitative assessment of dual gait analysis based on inertial sensors with body sensor network,” *Sensor Rev.*, vol. 33, no. 1, pp. 48–56, 2013.
- [12] R. Gravina, P. Alinia, H. Ghasemzadeh, and G. Fortino, “Multi-sensor fusion in body sensor networks: State-of-the-art and research challenges,” *Inf. Fusion*, vol. 35, pp. 68–80, May 2017.
- [13] J. Cao, W. Li, C. Ma, and Z. Tao, “Optimizing multi-sensor deployment via ensemble pruning for wearable activity recognition,” *Inf. Fusion*, vol. 41, pp. 68–79, May 2018.
- [14] W.-C. Cheng and D.-M. Jhan, “Triaxial accelerometer-based fall detection method using a self-constructing cascade-AdaBoost-SVM classifier,” *IEEE J. Biomed. Health Informat.*, vol. 17, no. 2, pp. 411–419, Mar. 2013.
- [15] J. Margarito, R. Helouai, A. M. Bianchi, F. Sartor, and A. G. Bonomi, “User-independent recognition of sports activities from a single wrist-worn accelerometer: A template-matching-based approach,” *IEEE Trans. Biomed. Eng.*, vol. 63, no. 4, pp. 788–796, Apr. 2016.
- [16] A. Wang, G. Chen, J. Yang, S. Zhao, and C.-Y. Chang, “A comparative study on human activity recognition using inertial sensors in a smartphone,” *IEEE Sensors J.*, vol. 16, no. 11, pp. 4566–4578, Jun. 2016.
- [17] D. Rodríguez-Martín, A. Samà, C. Pérez-López, J. Cabestany, A. Català, and A. Rodríguez-Moliner, “Posture transition identification on PD patients through a SVM-based technique and a single waist-worn accelerometer,” *Neurocomputing*, vol. 164, pp. 144–153, Sep. 2015.
- [18] Y. Fang, Z. Z. Yu, and J. C. Du, “A human activity recognition method based on a single inertial sensor,” in *Proc. Int. Conf. Adv. Educ. Technol. Inf. Eng.*, Beijing, China, May 2015, pp. 730–737.

- [19] K. N. K. A. Rahim, I. Elamvazuthi, L. I. Izhar, and G. Capi, "Classification of human daily activities using ensemble methods based on smartphone inertial sensors," *Sensors*, vol. 18, no. 2, 2018, Art. no. 4132.
- [20] M. Awais, L. Chiari, E. A. F. Ihlen, J. L. Helbostad, and L. Palmerini, "Physical activity classification for elderly people in free-living conditions," *IEEE J. Biomed. Health Informat.*, vol. 23, no. 1, pp. 197–207, Jan. 2019.
- [21] A. D. Ignatov and V. V. Strijov, "Human activity recognition using quasiperiodic time series collected from a single tri-axial accelerometer," *Multimedia Tools Appl.*, vol. 75, no. 12, pp. 7257–7270, 2016.
- [22] R. Akhaviani and A. H. Behzadan, "Smartphone-based construction workers' activity recognition and classification," *Autom. Construct.*, vol. 71, no. 2, pp. 198–209, Nov. 2016.
- [23] Z. Wang, D. Wu, R. Gravina, G. Fortino, Y. Jiang, and K. Tang, "Kernel fusion based extreme learning machine for cross-location activity recognition," *Inf. Fusion*, vol. 37, pp. 1–9, Sep. 2017.
- [24] D. Wu, Z. Wang, Y. Chen, and H. Zhao, "Mixed-kernel based weighted extreme learning machine for inertial sensor based human activity recognition with imbalanced dataset," *Neurocomputing*, vol. 190, pp. 35–49, May 2016.
- [25] C. Chen, W. Li, H. Su, and K. Liu, "Spectral-spatial classification of hyperspectral image based on kernel extreme learning machine," *Remote Sens.*, vol. 6, no. 6, pp. 5795–5814, 2014.
- [26] M. Wang, H. Chen, H. Li, Z. Cai, X. Zhao, C. Tong, and J. Li, and X. Xu, "Grey wolf optimization evolving kernel extreme learning machine: Application to bankruptcy prediction," *Eng. Appl. Artif. Intell.*, vol. 63, pp. 54–68, Aug. 2017.
- [27] W.-J. Niu, Z.-K. Feng, C.-T. Chen, and J.-Z. Zhou, "Forecasting daily runoff by extreme learning machine based on quantum-behaved particle swarm optimization," *J. Hydrologic Eng.*, vol. 23, no. 3, 2018, Art. no. 04018002.
- [28] Y. Chen, Z. Zhao, S. Wang, and Z. Chen, "Extreme learning machine-based device displacement free activity recognition model," *Soft Comput.*, vol. 16, no. 9, pp. 1617–1625, 2012.
- [29] Z. Chen, Q. Zhu, S. Y. Chai, and L. Zhang, "Robust human activity recognition using smartphone sensors via CT-PCA and online SVM," *IEEE Trans. Ind. Informat.*, vol. 13, no. 6, pp. 3070–3080, Dec. 2017.
- [30] A. M. Khan, Y.-K. Lee, S. Y. Lee, and T.-S. Kim, "A triaxial accelerometer-based physical-activity recognition via augmented-signal features and a hierarchical recognizer," *IEEE Trans. Inf. Technol. Biomed.*, vol. 14, no. 5, pp. 1166–1172, Sep. 2010.
- [31] W. Xiao and Y. Lu, "Daily human physical activity recognition based on kernel discriminant analysis and extreme learning machine," *Math. Problems Eng.*, vol. 2015, Nov. 2014, Art. no. 790412.
- [32] O. Banos, J.-M. Galvez, M. Damas, H. Pomares, and I. Rojas, "Window size impact in human activity recognition," *Sensors*, vol. 14, no. 4, pp. 6474–6499, Apr. 2014.
- [33] Y. Tian, X. Wang, L. Chen, and Z. Liu, "Wearable sensor-based human activity recognition via two-layer diversity-enhanced multiclassifier recognition method," *Sensors*, vol. 19, no. 9, 2019, Art. no. 2039.
- [34] G.-B. Huang, H. Zhou, X. Ding, and R. Zhang, "Extreme learning machine for regression and multiclass classification," *IEEE Trans. Syst., Man, Cybern. B, Cybern.*, vol. 42, no. 2, pp. 513–529, Apr. 2012.
- [35] G.-B. Huang, Q.-Y. Zhu, and C.-K. Siew, "Extreme learning machine: Theory and applications," *Neurocomputing*, vol. 70, nos. 1–3, pp. 489–501, 2006.
- [36] J. Sun, B. Feng, and W. Xu, "Particle swarm optimization with particles having quantum behavior," in *Proc. Congr. Evol. Comput.*, vol. 1, Jun. 2004, pp. 325–331.



YIMING TIAN received the B.S. degree in automation from the Hebei University of Technology, Tianjin, China, in 2012, and the M.S. degree in control science and control engineering from the University of Science and Technology at Liaoning, Anshan, China, in 2015. He is currently pursuing the Ph.D. degree in control science and control engineering with the Hebei University of Technology.

He is also a Research Assistant with the National Research Center for Rehabilitation Technical Aids. Since November 2018, he has been a Visiting Student with Newcastle University. His research interests include neural networks, wearable sensors, pattern recognition, and bioinformatics.



JIE ZHANG received the B.Sc. degree in control engineering from the Hebei University of Technology, Tianjin, China, in 1986, and the Ph.D. degree in control engineering from City, University of London, London, in 1991.

He is currently a Reader with the School of Engineering, Newcastle University, Newcastle upon Tyne, U.K. He has published over 290 papers in international journals, books, and conferences. His research interests include neural networks,

neuro-fuzzy systems, intelligent control systems, genetic algorithms, optimal control of batch processes, and multivariate statistical process control.

He is a member of the IEEE Control Systems Society, and the IEEE Computational Intelligence Society. He is on the Editorial Boards of a number of journals, including *Neurocomputing*, *PLOS ONE*, and the *International Journal of Automation and Computing*.



LINGLING CHEN was born in Zhangjiakou, Hebei, China, in 1981. She received the M.S. degree in control theory and control engineering and the Ph.D. degree from the Hebei University of Technology, Tianjin, China, in 2006 and 2010, respectively.

Since 2010, she has been with the Hebei University of Technology, where she is currently an Associate Professor. Her research interests include robot control, signal processing, and pattern recognition.



YANLI GENG received the B.S. degree in control technology and instruments from the Agricultural University of Hebei, Hebei, China, in 2006, and the M.S. and Ph.D. degrees in control theory and control engineering from the Hebei University of Technology, Tianjin, China, in 2009 and 2012, respectively.

She is currently a Lecturer with the School of Artificial Intelligence and Data Science, Hebei University of Technology. She is also with the Engineering Research Center of Intelligent Rehabilitation, Ministry of Education of China. Her research interests include rehabilitation engineering, intelligent control, and robotics.



XITAI WANG received the B.S. degree in automation from the Hebei University of Technology, Tianjin, China, and the M.S. degree in biomedical engineering from the Health Science Center, Peking University, Beijing, China.

He is currently a Professor and a Ph.D. Supervisor with the School of Artificial Intelligence and Data Science, Hebei University of Technology. He is also a Professor with the National Research Center for Rehabilitation Technical Aids. He has published more than 50 research papers. He has held several research grants from the National Key Technology Research and Development Program of the Ministry of Science and Technology of China as well as industry. His research interests include smart prostheses, specialized rehabilitation, intelligent control, body sensor networks, and computer networks.